

Honeycomb Sheet Structures Achieving High Electrical Conductivities in Alkyl-Substituted Thiazolium Bis(2-thioxo-1,3-dithiole-4,5-dithiolato)nickelate(III) Complex Salts

Etsuko Tomiyama,*[1,2] Kazuaki Tomono,[1] Daisuke Hashizume,[2] Tatsuo Wada,[2] and Kazuo Miyamura[1]

[1]Department of Chemistry, Faculty of Science, Tokyo University of Science, 1-3 Kagurazaka, Shinjuku-ku, Tokyo 162-8601

[2]RIKEN (The Institute of Physical and Chemical Research), 2-1 Hirosawa, Wako 351-0198

Received October 14, 2008; E-mail: j1306709@ed.kagu.tus.ac.jp

A series of $[Ni(dmit)_2]$ (**1**) (dmit = 2-thioxo-1,3-dithiole-4,5-dithiolato) complex salts with 3,4-dimethylthiazolium (**2**), 2,3,4-trimethylthiazolium (**3**), and 3,4,5-trimethylthiazolium (**4**) cations (**I**, **II**, and **III**, respectively) were synthesized and characterized by single-crystal X-ray analysis and conductivity. The molecular structures of **1** were the same in all three complex salts. In the structure of **I**, the anions were arranged in hexagonal structures. Neighboring hexagons formed honeycomb sheet structures as the result of S···S interactions in the (001) plane. The sheets of the honeycomb structures were arranged along the *c* axis with translational symmetries that form columnar honeycomb channels along the $[\bar{1}\bar{1}1]$ direction. In the structures of **II** and **III**, honeycomb sheet structures were formed as in **I**. But in contrast to **I**, the relative position of the stacked sheets in **II** and **III** was slightly dislocated, forming zig-zag channels instead. The IR spectra of **I**, **II**, and **III** show that the C=C stretching band is slightly red-shifted to 1337–1339 from 1350 cm^{-1} for $[Ni(dmit)_2]^-$, caused by the partial oxidation of the anion. The measured values of the electrical conductivities were 0.20, 0.094, and 0.16 $S\,cm^{-1}$ for **I**, **II**, and **III**, respectively. These high conductivities may be ascribed to the partially oxidation of the anion. The S···S interactions regulate the honeycomb sheet structure of the crystal and should work as conduction pathways effectively.

The metal–dithiolate complex is an excellent building block for electronic materials.[1,2] Transition-metal complexes of dmit (dmit = 2-thioxo-1,3-dithiole-4,5-dithiolato) have received significant attention since the report of the first open-shell molecular superconductor $(TTF)[Ni(dmit)_2]_2$ (TTF = tetrathiafulvalene)[3] and the first closed-shell molecular superconductor $[N(CH_3)_4][Ni(dmit)_2]_2$.[4] Although the closed-shell cations make no contribution to the conductivity, their size and shape play a predominant role in influencing the crystal structure, and consequently in altering the electronic properties. Physical properties of molecular conductors depend on the molecular alignment in crystals. Reefman et al.[5] reported the (tmiz)-$[Ni(dmit)_2]$ (tmiz = 1,2,3-trimethylimidazolium) salt featuring a type of cation that can be regarded as an intermediate between an open-shell and closed-shell cation. This compound showed a high conductivity of 0.21 $S\,cm^{-1}$ compared with other 1:1 $[Ni(dmit)_2]$ complex salts. (MeQ)$[Ni(dmit)_2]$ (MeQ = *N*-methylquinolinium) was characterized by single-crystal X-ray analysis and exhibited a conductivity of 10^{-3} $S\,cm^{-1}$.[6] These compounds crystallize in a non-segregated manner, displaying a face-to-face stacking mode of the anions and cations. These results suggested that the interaction between the π-electronic systems of both the cations and the anions might be responsible for the conductivity. We have already reported the crystal structure of the $[Ni(dmit)_2]$ complex salt with the 2,3-diethylthiazolium (**5**) cation.[7] In that crystal structure, S···S intermolecular interactions between the anions formed a distorted honeycomb structure parallel to the (001) plane, with cavities ≈12.34 Å in diameter. The cavities were filled with cations. The cations and anions linked via S···S and C–H···S interactions. To gain more insight into the regulated structures,[8,9] we have synthesized the dmit complex salts with three di- and trimethylthiazolium cations, whose molecular structures are similar to the dmit ligand. In this work, we have selected three cations for forming complex salts with $[Ni(dmit)_2]$ anion **1**; 3,4-dimethylthiazolium (abbreviated as 3,4-dmtz; **2**), 2,3,4-trimethylthiazolium (abbreviated as 2,3,4-tmtz; **3**), and 3,4,5-trimethylthiazolium (abbreviated as 3,4,5-tmtz; **4**) cations. Hereafter, the crystals of **1** and **2**, **1** and **3**, **1** and **4**, and **1** and **5** are abbreviated as **I**, **II**, **III**, and **IV**, respectively (Chart 1).

Experimental

Syntheses of (3,4-dmtz)$[Ni(dmit)_2]$ (I), (2,3,4-tmtz)$[Ni(dmit)_2]$ (II), and (3,4,5-tmtz)$[Ni(dmit)_2]$ (III). $(Bu_4N)[Ni(dmit)_2]$ was synthesized according to the literature.[10] 3,4-Dmtz iodide, 2,3,4-tmtz iodide, and 3,4,5-tmtz iodide were prepared by a similar procedure as follows: 4-methylthiazole, 2,4-dimethylthiazole, or 4,5-dimethylthiazole (20 mmol) and methyl iodide (100 mmol) were stirred in Et_2O (30 mL) for two days. The resultant solid was filtered and washed several times with acetone and Et_2O to obtain derivatives of each methylthiazolium iodide. All reagents were of reagent grade and used without further purification. Single crystals were prepared by the cation-exchange method and slow inter-

Published on the web March 12, 2009; doi:10.1246/bcsj.82.352

diffusion of acetonitrile solution (25 mL) of $(Bu_4N)[Ni(dmit)_2]$ (0.05 mol) and chloroform/methanol (15:1) solution (45 mL) of 3,4-dmtz iodide (0.1 mol), 2,3,4-tmtz iodide (0.1 mol), or 3,4,5-tmtz iodide (0.1 mol) for several days at room temperature.

Elemental analyses and IR spectra: (3,4-dmtz)$[Ni(dmit)_2]$ (**I**): Anal. Found: C, 23.60; H, 1.13; N, 2.45%. Calcd for $C_{11}H_8NS_{11}Ni$: C, 23.36; H, 1.43; N, 2.48%. IR (KBr, cm^{-1}): 3106 (w), 1575 (w), 1338 (s, C=C), 1233 (w), 1169 (w), 1065 (s, C=S). (2,3,4-tmtz)$[Ni(dmit)_2]$ (**II**): Anal. Found: C, 25.00; H, 1.42; N, 2.40%. Calcd for $C_{12}H_{10}NS_{11}Ni$: C, 24.87; H, 1.74; N, 2.42%. IR (KBr, cm^{-1}): 3120 (w), 1589 (w), 1337 (s, C=C), 1246 (w), 1186 (w), 1065 (s, C=S). (3,4,5-tmtz)$[Ni(dmit)_2]$ (**III**): Anal. Found: C, 25.05; H, 1.42; N, 2.41%. Calcd for $C_{12}H_{10}NS_{11}Ni$: C, 24.87; H, 1.74; N, 2.42%. IR (KBr, cm^{-1}): 3073 (w), 1595 (w), 1339 (m, C=C), 1260 (w), 1196 (w), 1062 (m and br, C=S).

X-ray Crystallography. Diffraction data of **I**, **II**, and **III** were collected with a Bruker AXS SMART diffractometer equipped with CCD area detector using Mo Kα ($\lambda = 0.71073$ Å) radiation. The structures of **I**, **II**, and **III** were solved and refined using the programs SHELXS-97 and SHELXL-97,[11] respectively. All non-hydrogen atoms were refined anisotropically. Positions of hydrogen atoms were calculated geometrically, and refined as riding models. Crystallographic data are listed in Table 1. Crystallographic data have been deposited with Cambridge Crystallographic Data Centre: Deposition numbers CCDC-704658, -704659, and -704660 for compounds **I**, **II**, and **III**, respectively. Copies of the data can be obtained free of charge via http://www.ccdc.cam.ac.uk/conts/retrieving.html (or from the Cambridge Crystallographic Data Centre, 12, Union Road, Cambridge, CB2 1EZ, U.K.; Fax: +44 1223 336033; e-mail: deposit@ccdc.cam.ac.uk).

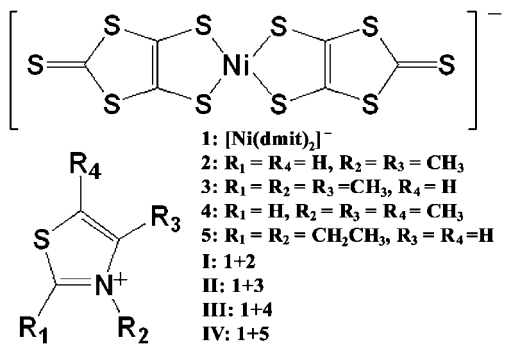

Chart 1.

Measurements. IR spectra (KBr pellets) were measured using a JASCO FT/IR-410 spectrophotometer. Elemental analyses were performed with a Perkin-Elmer 2400II CHN analyzer. Conductivity measurements were carried out at ambient pressure using a two-probe ac impedance method. Electrical contacts were prepared using silver paste to attach 0.1 mmϕ gold wires (The Nilaco CORPORATION) to the crystals. The magnitude of the applied potential was 1 V in the (001) plane.

Results and Discussion

IR Measurement. The strong bands around 1350 cm^{-1} in the IR spectra assigned to the C=C stretching band is known to exhibit a large shift because of the formal charge of $Ni(dmit)_2$; 1260 cm^{-1} for $[Ni(dmit)_2]^{0.29-}$, 1350 cm^{-1} for $[Ni(dmit)_2]^-$, and 1440 cm^{-1} for $[Ni(dmit)_2]^{2-}$.[12] Three crystals of **I**, **II**, and **III** were 1:1 complex salts supported by elemental analyses and crystal structure analyses. IR spectra, on the other hand, show that the C=C stretching band has a slight red shift (1337–1339 cm^{-1}) from the expected value of 1350 cm^{-1} for $[Ni(dmit)_2]^-$. This suggests that the formal charge of $[Ni(dmit)_2]$ anions in **I**, **II**, and **III** has shifted to less negative values. In the case of **IV**, the spectra has the expected C=C stretching band at 1353 cm^{-1}, indicating that $[Ni(dmit)_2]$ anion in **IV** has a formal charge of -1.[12]

Molecular Structures. ORTEP plots with the atomic numbering scheme of the four molecules **1**, **2**, **3**, and **4** are given in Figure 1. The crystals of **I**, **II**, and **III** include one crystallographically independent **1** and one counter cation within the asymmetric units. There are no significant geometrical differences in the structures of **1** among these crystals. The structures of **1** in the salts are almost planar within 0.0856(11), 0.0598(17), and 0.0424(10) Å for **I**, **II**, and **III**,

Table 1. Crystallographic Data of Complex Salts **I**, **II**, and **III**

	I	**II**	**III**
Formula	$C_{11}H_8NNiS_{11}$	$C_{12}H_{10}NNiS_{11}$	$C_{12}H_{10}NNiS_{11}$
FW	565.55	579.58	579.58
Crystal system	Triclinic	Triclinic	Triclinic
Space group	$P\bar{1}$	$P\bar{1}$	$P\bar{1}$
a/Å	8.7476(6)	7.8987(11)	7.9774(7)
b/Å	9.5979(6)	10.5342(15)	10.5219(9)
c/Å	12.8223(8)	13.4853(19)	13.2822(11)
α/°	77.5520(10)	71.029(2)	71.6350(10)
β/°	86.4570(10)	82.029(2)	80.880(2)
γ/°	75.4880(10)	78.393(2)	77.708(2)
V/Å^3	1017.66(11)	1036.2(3)	1028.80(15)
Z	2	2	2
D_X/Mg m^{-3}	1.846	1.858	1.871
μ/mm^{-1}	2.078	2.043	2.058
S	1.07	1.02	0.92
$R(F)$[a] [refs. $I > 2\sigma(I)$]	0.033	0.046	0.034
$wR(F^2)$[b] [refs. $I > 2\sigma(I)$]	0.097	0.134	0.092
$\Delta\rho_{min,max}$/e Å^{-3}	−0.68, 0.41	−0.68, 1.01	−0.44, 0.36

a) $R(F) = \Sigma||F_o| - |F_c||/\Sigma|F_o|$. b) $wR(F^2) = \Sigma[w(F_o^2 - F_c^2)^2]/\Sigma[w(F_o^2)^2]^{1/2}$.

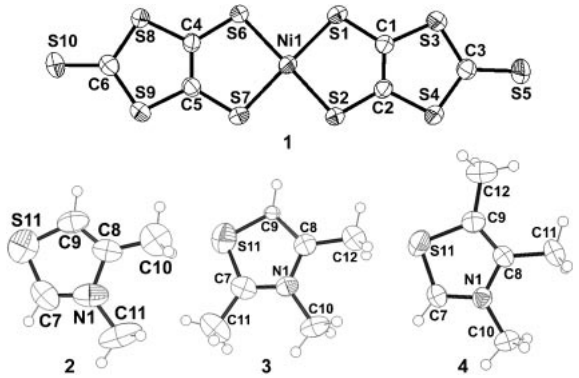

Figure 1. ORTEP views of **1**, **2**, **3**, and **4** showing 50% probability ellipsoids and the atom-numbering scheme.

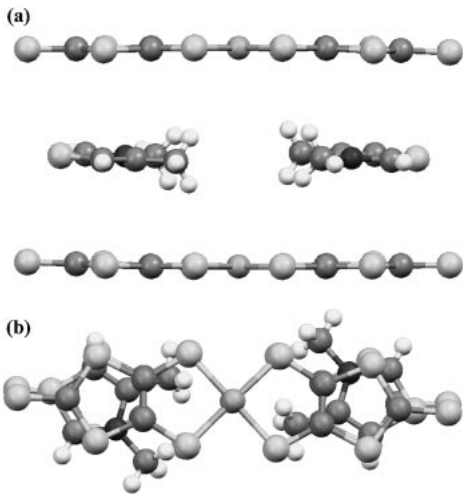

Figure 2. Stacking of **1** and **2** in **I**; (a) side view and (b) top view.

respectively. In these crystals, the Ni–S distances range from 2.1504(11) to 2.1731(19) Å, with an average of 2.160 Å, and the *cis*-S–Ni–S angles range from 85.76(3) to 93.43(3)°; the NiS_4 coordination thus adopts a slightly distorted square-planar configuration. The coordinated dmit ligands are coplanar with each other; the dihedral angles between them are 2.04(5), 0.74(7), and 0.30(6)° for **I**, **II**, and **III**, respectively. The dihedral angles between the thiazole ring of the cations and the molecular plane of the anions are 4.38(14), 1.51(19), and 1.24(18)° for **I**, **II**, and **III**, respectively. The thiazole rings are almost planar within 0.0059(16), 0.0060(23), and 0.0043(19) Å for **I**, **II**, and **III**, respectively, and the carbons of the methyl groups on the thiazole rings are also on the thiazole plane within 0.035(5) [C10] and 0.025(6) Å [C11] for **I**, 0.001(7) [C10], 0.023(7) [C11], and 0.029(7) Å [C12] for **II**, and 0.024(5) [C10], 0.003(6) [C11], and 0.046(6) Å [C12] for **III**. The double bond lengths (N1–C7 and C8–C9) in the thiazole ring are 1.362(5) and 1.329(5) Å for **I**, 1.321(6) and 1.461(5) Å for **II**, 1.342(4) and 1.351(5) Å for **III**, respectively.

Crystal Structure of I. The crystal contained a crystallographically independent pair of **1** and **2**. These two anions sandwiched the cations (Figure 2a); the molecules of **2** stacked on the dmit moieties with alignment of the molecular shapes (Figure 2b). The distances between the centroids of the dmit

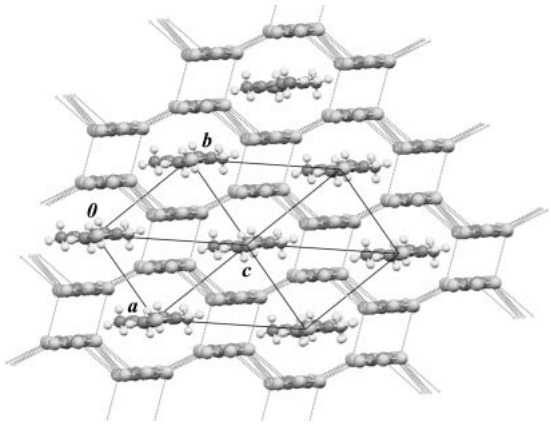

Figure 3. Crystal structure of **I**, showing honeycomb structure in the (001) plane, viewed along the molecular axis of **1**. S···S interactions are shown by dashed lines.

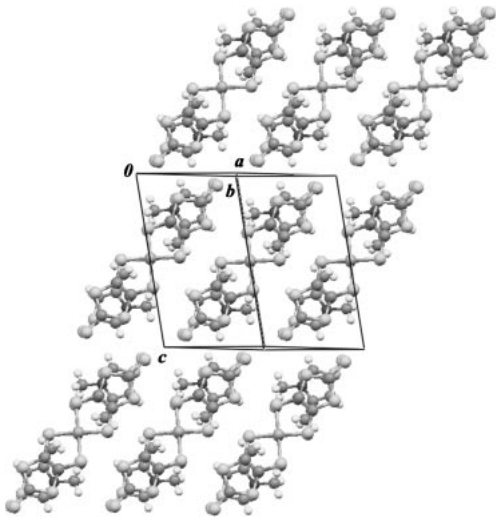

Figure 4. Three sheets of honeycomb structures stacked along the *c* axis with the translational symmetries.

(C1–C2–S4–C3–S3) and thiazole rings (N1–C8–C9–S11–C7) were approximately 3.851 and 3.768 Å, which are enough to close to form four π–π interactions.[13] These anions are arranged into a hexagonal structure in the (001) plane. Neighboring hexagons are joined together with sharing of all edges to form a honeycomb sheet structure (Figure 3). The sheets of the honeycomb structures are arranged along the *c* axis with the translational symmetries producing the columnar honeycomb structures, which have straight channels along the $[\bar{1}\bar{1}1]$ direction (Figure 4). The cations are placed in the channels. This columnar honeycomb structure is regulated by many S···S interactions. The S···S distances shorter than 3.70 Å, the sum of the van der Waals radii of S atoms, are listed in Table 2. In addition, two C–H···S and four π–π interactions between cations and anions are also close enough to contribute to the honeycomb columnar structures (Table 3).

Crystal Structures of Isostructural II and III. The molecules of **3** and **4** are structural isomers of each other (see Figure 1), and exhibit isostructural crystal packing. As shown in Figures 5a and 5c, two anions sandwiched two cations in **II**

and **III**. Figures 5b and 5d show that the relative orientations between the anions and cations are almost the same in each crystal: three methyl groups and a sulfur atom (S11) occupy the same positions. A slight difference is the location of each N1 atom. The distances between the centroids of the dmit (C1–C2–S4–C3–S3) and thiazole rings (N1–C8–C9–S11–C7) are about 3.643 and 4.531 Å in **II** and 3.631 and 4.499 Å in **III**. In contrast to **I**, overlaps of thiazole rings with dmit are small. These anions are arranged to form the hexagonal structure. Neighboring hexagons are joined together with sharing of all edges to form a honeycomb sheet structure in the (001) plane (Figures 6a and 6d) as in **I**. The sheets are stacked along the *c* axis by the translational symmetries (Figures 6b and 6e). The relative position of the stacked sheets is slightly dislocated, thus zigzag channels are formed in **II** and **III** (Figures 6c and 6f). The honeycomb structures are regulated by many S···S interactions. The corresponding S···S distances are listed in Table 4. In addition, two C–H···S and two π–π interactions are found between cations and anions (Table 5).

Table 2. Distances/Å of S···S Interactions in **I**

	I
S1···S7[a)]	3.6610(10)
S1···S8[b)]	3.6803(9)
S2···S2[c)]	3.5524(13)
S2···S4[c)]	3.5410(10)
S4···S7[c)]	3.5765(10)
S5···S10[d)]	3.4816(12)
S6···S6[b)]	3.5909(12)
S6···S8[b)]	3.4010(9)
S9···S10[e)]	3.6504(11)

Symmetry codes: a) $2-x$, $-y$, $1-z$; b) $2-x$, $1-y$, $1-z$; c) $2-x$, $-y$, $1-z$; d) $-1+x$, $-1+y$, $1+z$; e) $2-x$, $1-y$, $-z$.

Table 3. Geometries of Possible C–H···S Hydrogen Bonds in **I**

D–H···A	D–H/Å	H···A/Å	D···A/Å	(D–H···A)/°
C10–H10B···S1	0.96	2.97	3.869(4)	156
C7–H7···S10[a)]	0.93	2.96	3.817(4)	154

a) Symmetry code: $-1+x$, y, $1+z$.

Electrical Conductivities. The values of the conductivities in the (001) planes were 0.20, 0.094, and 0.16 S cm^{-1} for **I**, **II**, and **III**, respectively. These conductivities of **I**, **II**, and **III** are unexpectedly high among the series of Z[Ni(dmit)$_2$] of 1:1 complexes. In the crystal structures of **I**, **II**, **III**, and **IV** similar honeycomb sheet structures are formed in the (001) plane. The high conductivities of **I**, **II**, and **III** suggest that the honeycomb sheets may contribute to the conduction pathways. However, as reported previously the electrical conductivity of **IV** was

Table 4. Distances/Å of S···S Interactions in **II** and **III**

	II	**III**
S1···S1[a)]	3.637(2)	3.6600(19)
S1···S3[a)]	3.5924(17)	3.5778(14)
S2···S9[b)]	3.6747(16)	3.6890(13)
S3···S6[a)]	3.6252(16)	3.6273(14)
S4···S6[c)]	(3.7319(17))	3.6992(14)
S4···S11[d)]	3.6328(18)	3.5681(14)
S5···S5[e)]	(3.724(2))	3.676(2)
S5···S11[d)]	3.586(2)	3.6176(15)
S7···S7[b)]	3.555(2)	3.5410(17)
S8···S8[f)]	3.365(2)	3.3496(18)

Symmetry codes: a) $-x$, $-y$, $2-z$; b) $1-x$, $1-y$, $2-z$; c) $1-x$, $-y$, $2-z$; d) x, $-1+y$, $1+z$; e) $-x$, $-1-y$, $3-z$; f) $1-x$, $1-y$, $1-z$.

Table 5. Geometries of Possible C–H···S Hydrogen Bonds in **II** and **III**

D–H···A	D–H/Å	H···A/Å	D···A/Å	(D–H···A)/°
II				
C10–H10A···S1[a)]	0.96	2.97	3.694(5)	134
C12–H12B···S3[b)]	0.96	2.98	3.883(5)	158
III				
C10–H10C···S3[b)]	0.96	2.94	3.787(4)	148
C11–H11A···S1[a)]	0.96	2.91	3.734(4)	145

Symmetry codes: a) x, $1+y$, z; b) $-x$, $-y$, $2-z$.

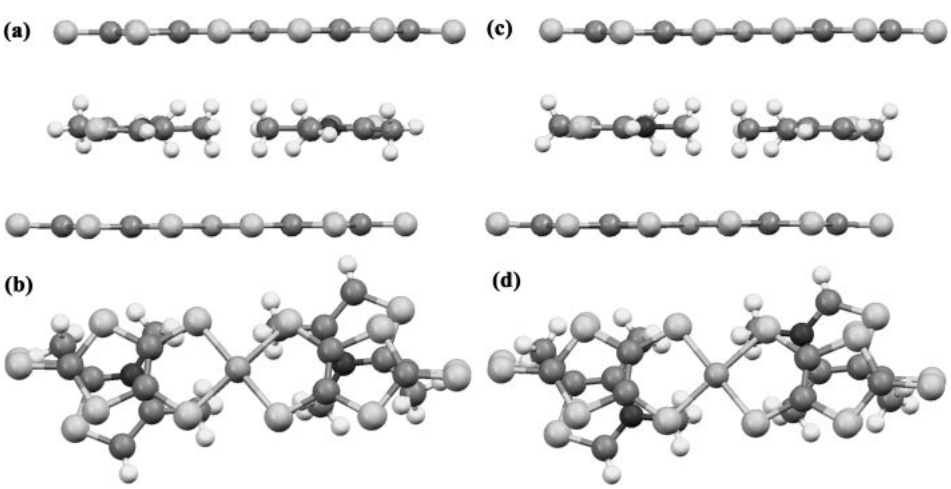

Figure 5. Stacking of **1** and **3** in **II**; (a) side view and (b) top view. Stacking of **1** and **4** in **III**; (c) side view and (d) top view.

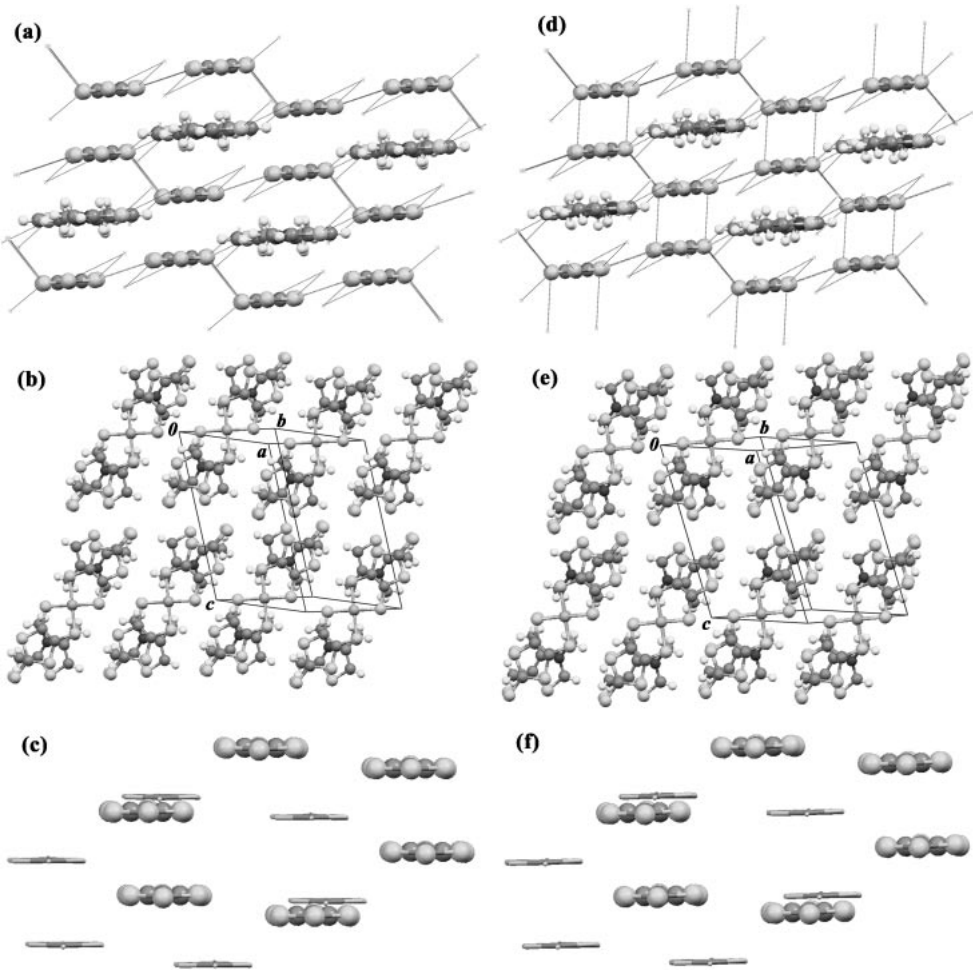

Figure 6. Packing motifs of **II** and **III**. (a) Sheet of honeycomb structure in the (001) plane; (b) two sheets of honeycomb structures stacked along the *c* axis with the translational symmetries; (c) hexagons in the honeycomb structure shown by ball-and-stick anions in front, and capped sticks behind for **II**. Figures d, e, and f correspond to those for **III**.

Table 6. Numbers of S···S Interactions Classified by Stacking Configurations in **I**, **II**, **III**, and **IV**

	I	II	III	IV
Intra-honeycomb sheet				
face-to-face	1	[1][a)]	1	[2][a)]
side-by-side	6	5	5	1 + [4][a)]
anion–cation				2
Inter-honeycomb sheet				
head-to-head	1	[1][a)]	1	1
side-by-side	1	1	1	
anion–cation		1	1	

a) S···S separation distance of 3.7–3.8 Å (sum of the van der Waals radii of S atoms is 3.7 Å).

10^{-7} cm^{-1}, which is not high at all,[7] suggesting that the molecular interactions in the (001) plane should be slightly different in all four complexes. Table 6 shows the numbers of S···S distances classified by the stacking configuration shown in Figure 7. In the honeycomb sheet, face-to-face stackings are attributed to the large molecular orbital transfer, and side-by-

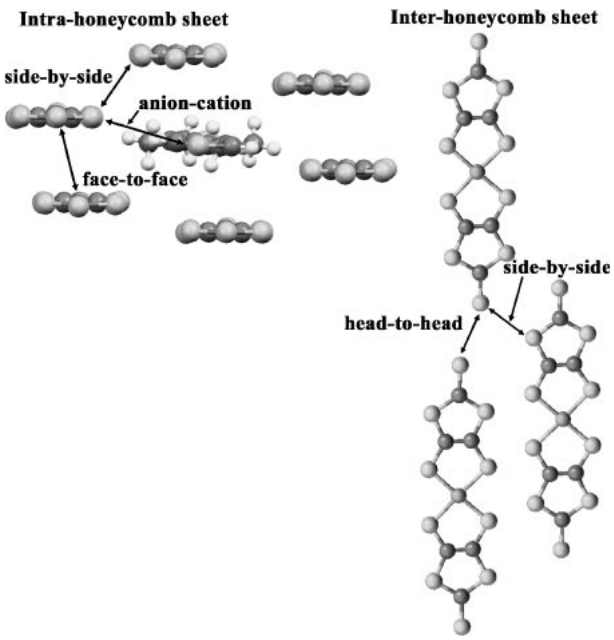

Figure 7. Stacking configurations of anions within the intra- and inter-honeycomb sheets.

side stackings are less effective to the conduction pathway due to small molecular orbital transfer. The honeycomb structures of **I** and **III**, on the other hand, have face-to-face stacking and many side-by-side stackings; those of **II** have no face-to-face stacking, but many side-by-side stackings, similar to **I** and **III**. The distorted honeycomb sheet structure of **IV** had no short face-to-face stacking, and has a small number of side-by-side stacking. The short face-to-face and side-by-side stacking promote regular honeycomb structures. Between honeycomb sheets, almost the same numbers of S···S interactions exist, and these interactions contribute to the formation of crystal structures for all four complexes. However, the overlapping of π-orbitals for inter-sheets S···S interactions is quite small. These interactions do not contribute to electrical conductivity. We believe that the regularity of the honeycomb hexagons is an important factor in archiving high conductivities, while the distorted honeycomb hexagons as in **IV** seem to favor low conductivity. As previously mentioned, the IR spectra provide compelling evidence that the formal charge of the anion is shifted to less negative values, and thus shift seems to correlate with the degree of regularity of the honeycomb hexagons. Therefore, the partially auto-oxidized formal charge of the $[Ni(dmit)_2]$ anion is a factor that must be taken into consideration to explain the high conductivity values.

Conclusion

We have prepared three 1:1 complex salts composed of $[Ni(dmit)_2]$ anion and di- or trimethyl-substituted thiazolium cations that have high electrical conductivities, which are attributed to the auto-oxidation of anions and many S···S interactions that provide a conduction pathway in the crystals. The IR spectra confirms that the formal charge of the $[Ni(dmit)_2]$ anion has a slight positive shift from -1. Our crystallographic measurements reveal that the molecular structures of **1** were the same in all three complex salts studied, and furthermore in the structure of **I**, **II**, and **III**, the anions were arranged to form hexagonal patterns, and neighboring hexagons formed honeycomb sheet structures as a result of S···S interactions. The honeycomb structures of **I** and **III** have face-to-face stacking and many side-by-side stackings; those of **II** have no face-to-face stacking, but do have many side-by-side stackings, similar to **I** and **III**. The sheets of the honeycomb structures in **I** were stacked to form a columnar cation channel. In the honeycomb sheet structures of **II** and **III**, the distortion of the hexagonal pattern, results in the cations being aligned in a zig-zag pattern along $[\bar{1}\bar{1}1]$ direction. The values of the electrical conductivities for **I**, **II**, and **III** were 0.20, 0.094, and 0.16 $S\,cm^{-1}$, respectively. These high conductivities may be attributed to the partial auto-oxidation of the anions, as well as the regularity of the honeycomb sheet structure. In the latter case, the hexagonal sheets provide a 2-D conductivity path for the electrons, while to a lesser extent the S···S interactions between sheets may contribute to the conduction pathways.

Finally, these dmit salts used in this study are easily synthesized on a large scale, and thus are attractive candidates for molecular design of conductors in industrial applications.

The authors thank Mr. Totsuka and Prof. Furukawa for performing the conductivity measurements.

Supporting Information

IR spectra of **I**, **II**, **III**, and **IV**, and experimental detail of electrical conductivities. This material is available free of charge on the Web at: http://www.csj.jp/journals/bcsj/.

References

1 H. V. Huynh, C. Schulze-Isfort, W. W. Seidel, T. Lugger, R. Frohlich, O. Kataeva, F. E. Hahn, *Chem.—Eur. J.* **2002**, *8*, 1327.
2 N. Robertson, L. Cronin, *Coord. Chem. Rev.* **2002**, *227*, 93.
3 M. Bousseau, L. Valade, J. P. Legros, P. Cassoux, M. Garbauskas, L. V. Interrante, *J. Am. Chem. Soc.* **1986**, *108*, 1908.
4 A. Kobayashi, H. Kim, Y. Sasaki, R. Kato, H. Kobayashi, S. Moriyama, Y. Nishio, K. Kajita, W. Sasaki, *Chem. Lett.* **1987**, 1819.
5 D. Reefman, J. P. Cornelissen, J. G. Haasnoot, R. A. G. de Graaff, J. Reedijk, *Inorg. Chem.* **1990**, *29*, 3933.
6 J. P. Cornelissen, E. J. Creyghton, R. A. G. de Graaff, J. G. Haasnoot, J. Reedijk, *Inorg. Chim. Acta* **1991**, *185*, 97.
7 E. Tomiyama, K. Tomono, K. Miyamura, *Acta Crystallogr., Sect. E* **2007**, *63*, M2741.
8 K. Tomono, K. Miyamura, *Chem. Lett.* **2007**, *36*, 1466.
9 K. Tomono, K. Ogawa, Y. Sasaki, K. Miyamura, *Inorg. Chim. Acta* **2008**, *361*, 269.
10 G. Steimecke, H. J. Sieler, R. Kirmse, E. Hoyer, *Phosphorous, Sulfur Silicon Relat. Elem.* **1978**, *7*, 49.
11 *SHELXS-97* and *SHELXL-97*: G. M. Sheldrick, *Acta Crystallogr., Sect. A* **2008**, *64*, 112.
12 L. Valade, J.-P. Legros, M. Bousseau, P. Cassoux, M. Garbaskas, L. V. Interrante, *J. Chem. Soc., Dalton Trans.* **1985**, 783.
13 C. Janiak, *J. Chem. Soc., Dalton Trans.* **2000**, 3885.